Title

Marine hydroid perisarc: A chitin- and melanin-reinforced composite with DOPA–iron(III) complexes

Journal

Acta Biomaterialia, 9(9)

ISSN

1742-7061

Authors

Hwang, Dong Soo
Masic, Admir
Prajatelistia, Ekavianty
et al.

Publication Date

2013-09-01

DOI

10.1016/j.actbio.2013.06.015

Peer reviewed

Acta Biomaterialia 9 (2013) 8110–8117

Contents lists available at SciVerse ScienceDirect

Acta Biomaterialia

journal homepage: www.elsevier.com/locate/actabiomat

Marine hydroid perisarc: A chitin- and melanin-reinforced composite with DOPA–iron(III) complexes

Dong Soo Hwang [a,b,c,*], Admir Masic [d], Ekavianty Prajatelistia [b], Mihaela Iordachescu [c], J. Herbert Waite [e,*]

[a] School of Environmental Science and Engineering, Pohang University of Science and Technology, Pohang 790-784, South Korea
[b] School of Interdisciplinary Bioscience and Bioengineering, Pohang University of Science and Technology, Pohang 790-784, South Korea
[c] POSTECH Ocean Science and Technology Institute, Pohang University of Science and Technology, Pohang 790-784, South Korea
[d] Department of Biomaterials, Max Planck Institute of Colloids and Interfaces, 14424 Potsdam-Golm, Germany
[e] Marine Science Institute, University of California, Santa Barbara, CA 93106, USA

ARTICLE INFO

Article history:
Received 5 March 2013
Received in revised form 7 June 2013
Accepted 10 June 2013
Available online 19 June 2013

Keywords:
Hydroid
Perisarc
DOPA
Chitin
DOPA–iron(III) complex

ABSTRACT

Many marine invertebrates utilize biomacromolecules as building blocks to form their load-bearing tissues. These polymeric tissues are appealing for their unusual physical and mechanical properties, including high hardness and stiffness, toughness and low density. Here, a marine hydroid perisarc of *Aglaophenia latirostris* was investigated to understand how nature designs a stiff, tough and lightweight sheathing structure. Chitin, protein and a melanin-like pigment, were found to represent 10, 17 and 60 wt.% of the perisarc, respectively. Interestingly, similar to the adhesive and coating of marine mussel byssus, a DOPA (3,4-dihydroxyphenylalanine) containing protein and iron were detected in the perisarc. Resonance Raman microprobe analysis of perisarc indicates the presence of catechol–iron(III) complexes in situ, but it remains to be determined whether the DOPA–iron(III) interaction plays a cohesive role in holding the protein, chitin and melanin networks together.

1. Introduction

Given their lightweight and excellent mechanical properties, mineral-deficient load-bearing tissues of marine invertebrate organisms (squid beaks and polychaete jaws) have attracted attention as high-performance biomaterials [1–4]. In contrast to vertebrate hard tissues, which are highly mineralized (>70% by dry mass), several marine-derived hard tissues contain significantly less mineral (<10% by dry mass) [5] but maintain comparable mechanical properties to those of their highly mineralized counterparts in vertebrates [5,6]. In addition, the marine environment has much in common with body fluids; both systems are naturally saline and experience variations of fluid flow and temperature, are prone to surface fouling via macromolecules, and exhibit cell-mediated catabolism and turnover of circulating organic solutes. A deeper understanding of the structure–function relationships in the hard tissues of marine organisms is considered by many to be a valuable database for designing lightweight and biocompatible materials for biomedical applications.

Previously studied mineral-deficient load-bearing fang-like jaws from two marine polychaetes (*Glycera* and *Nereis* species) are appropriate specific examples. Both jaws have similar shapes and mechanical properties that resemble those of human dentin but without a similar reliance on mineral. *Glycera* jaws consist of melanin (~37 dry wt.%), protein (~50%), copper-based minerals and metal ions (up to 10%), whereas *Nereis* jaws are a composite of halogenated proteins (70–90% of the total dry mass) and metal ions [1,4,6–10]. Melanin, which is usually associated with pigmentation, has significant load-bearing properties in *Glycera* jaw [2]. In contrast, in *Nereis* jaw, the metal coordination complex between zinc ions and the histidine-rich proteins, and dityrosine cross-links are the only known cohesive mechanisms underlying the observed hardness and stiffness of the jaws [8].

Another invertebrate structure appropriate for consideration is the beak of the jumbo squid (*Dosidicus gigas*). *Dosidicus* beak is composed entirely of organic molecules, which are chitin, histidine- and glycine-rich proteins, and catecholic pigments with 3,4-dihydroxyphenylalanine (DOPA) and 4-methylcatechol. Stiffness at the tip of the beak approaches a maximum of 5 GPa under wet conditions, which is achieved by a functional gradient, i.e. an increase in the density of catechol-based cross-linking of the histidine-rich proteins [3,11,12]. The stiffness of the completely non-mineralized beak of squid approaches that of the tooth dentin under wet conditions [3]. The stiffness of fully dried, anisotropic, crystalline α-chitin measured by X-ray diffraction was about

* Corresponding authors. at: School of Environmental Science and Engineering, Pohang University of Science and Technology, Pohang 790-784, South Korea. Tel.: +82 54 279 9505; fax: +82 54 279 9519 (D.S. Hwang). Tel.: +1 805 893 2817; fax: +1 805 893 7998 (J.H. Waite).

E-mail addresses: dshwang@postech.ac.kr (D.S. Hwang), waite@lifesci.ucsb.edu (J.H. Waite).

1742-7061/$ - see front matter © 2013 Acta Materialia Inc. Published by Elsevier Ltd. All rights reserved.
http://dx.doi.org/10.1016/j.actbio.2013.06.015

40 GPa [3,12,13], but that of fully hydrated chitin was gel-like, at less than 0.3 GPa (unpublished data). As previously described in *Dosidicus* beak, chitin provides a supporting framework for the catechols and proteins, which are ultimately responsible for the stiffening effect under fully hydrated conditions [12].

A chemically similar reaction has been reported in the perisarc of the hydroid *Laomedea flexuosa* [14–16]. The perisarc of hydroids is a sheath of chitin, proteins and inorganics that protect the main stalk and soft tissues. Preliminary histochemical studies reported that hydroid perisarc was composed of chitin fibers embedded in a mixture of proteins and dopamine (a catechol) oxidized by phenoloxidase [14,15]. This sounds remarkably reminiscent of the mechanism of beak hardening in *Dosidicus* even though the two organisms are phylogenetically separated, i.e. Cnidaria and Mollusca.

To more deeply explore this superficial resemblance, we further analyzed the biochemical and physical properties of hydroid perisarc in *Aglaophenia latirostris* Nutting, 1900 and ostrich-plume hydroid (phylum: Cnidaria; class: Hydrozoa; order: Hydroida), a common species on rocks or brown algae in the epibenthic zone extending from Southern Alaska to the central coast of California. Our results suggest that metal coordination, melanin formation and catechol-based cross-linking of proteins occur within a chitin mesh and play a role in the maturation of hydroid perisarc.

2. Materials and methods

2.1. Biochemical analysis

Live local hydroids (*A. latirostris*) used for this study were collected from Goleta Pier (Goleta, CA). Prior to chemical analysis, the hydroids were frozen in a deep-freezer, where they were stored at −80 °C until use. To separate the perisarc from the soft tissue and the impurities of seawater, harvested hydroids were incubated in 4 M urea/5% acetic acid solution for 48 h and washed thoroughly with deionized water. The hydroid perisarcs were freeze-dried and their dry weight recorded. The dried perisarcs were ground to powder with a mortar and pestle. The determination of the content of inorganics in hydroid perisarc was performed by mass weighing of freeze-dried hydroid before and after incubating in an oven at 450 °C for 24 h to remove the organic phase. Extraction of total lipid from the hydroid perisarc was performed in a mixture of methanol and chloroform, and the lipid content was determined by a previously reported method [17]. Total protein content was obtained independently by the Lowry method and by amino acid analysis after sample preparation by acid hydrolysis [11]. Carbohydrate and glycogen were extracted in 15% trichloroacetic acid from the ground hydroid perisarc and their contents determined by the phenol–sulfuric acid method. The content of chitin was independently determined by amino acid analysis. To isolate chitin from the perisarc, the perisarcs were treated with 7 wt.% HCl for 2 days at room temperature and then boiled in a 5 wt.% KOH solution for 2 days to remove residual proteins. To remove pigments in the sample, the sample was filtered and washed with distilled water.

2.2. Amino acids and chitin analysis

Hydroid polyps were freeze-dried, weighed and placed in hydrolysis vials with 6 M HCl and 5% phenol as antioxidant. The tubes were vacuum-sealed and heated at 110 °C for 2 days. The supernatant was then separated from the solid residue by centrifugation, flash-evaporated and analyzed in a ninhydrin-based SYKAM analyzer (SYKAM, Germany). The amino acid (AA) concentrations were calibrated using external standards. The presence of the catecholic compounds was tested by the Arnow assay [18]. To separate DOPA and other catecholic compounds, hydroid polyp samples were hydrolyzed at 156 °C for 1 h and, following flash evaporation, bound to a phenyl boronate affinity column [19] and washed with three column volumes of 0.1 M phosphate (pH 7.5) before eluting with 5 vol.% acetic acid. The fraction purified by phenyl-borate column was separated by high-performance liquid chromatography and analyzed by electrospray ionization–mass spectrometry (ESI-MS) using an AB SCIEX API 2000 mass spectrometer (Waters Corp., Milford, MA). The AA compositions of the eluting fractions were also analyzed as above. The chitin mass fraction was obtained from mass changes of freeze-dried hydroid polyp samples following a deproteinization/depigmentation treatment. Freeze-dried hydroid polyp samples in the alkaline peroxide cocktail (0.25 N NaOH and 1.5% (w/v) of H_2O_2) were incubated for 1 day at 50 °C [9]. Insoluble fraction was separated by the centrifugation, briefly washed with deionized water and freeze-dried. Freeze-dried insoluble fraction was hydrolyzed at 110 °C for 2 days and injected into the AAAA analyzer. Glucosamine hydrochloride (GA-HCl, the hydrolysis product of chitin when subjected to 6 M HCl) was used as an external standard for chitin content calculation [11].

2.3. Melanin-like pigment characterization and quantification

Melanin-like pigment characterization and quantification in non-hydrolyzable part of Aglaophenia perisarc after acid hydrolysis was carried out by alkaline peroxidation, X-ray photoelectron spectroscopy (XPS) and infrared spectroscopy (IR) [19]. *Sepia* melanin (Sigma) was used as a standard, with concentrations of 0, 0.1, 0.2, 0.5 and 1 mg ml^{-1}. The hydrolyzed and non-hydrolyzed samples were then checked by the alkaline peroxidation method. As the hydrolyzed sample, the freeze-dried hydroid and *Sepia* melanin were weighed and placed in hydrolysis vials with 6 M HCl and 5% phenol as antioxidant. The vials were vacuum-sealed and heated at 110 °C for 2 days. The insoluble residues were separated from the supernatant by centrifugation, washed with distilled water and methanol to remove HCl, then fully dried in a convection oven. Non-hydrolyzable insoluble residues were compressed into a KBr pellet. IR adsorption and XPS spectra of the pellet were measured using a Fourier transform infrared spectrometer (Excalibur, Bio Rad, Hercules, CA) with a resolution of 4 cm^{-1} in the wavenumber region of 700–4000 cm^{-1} and an X-ray photoelectron spectrometer (PHI 5800 ESCA System, Philips, Netherlands), respectively. Non-hydrolyzable insoluble residues also were suspended as 0, 0.1, 0.2, 0.5 and 1 mg ml^{-1} solutions in alkaline peroxide cocktail (1 vol. of 10 N NaOH, 2 vols. of 30% H_2O_2, 37 vols. of deionized water), then analyzed for absorbance at 560 nm to determine the total melanin content. After the mixtures were incubated overnight at 70 °C and centrifuged at 14,000 rpm to remove residual solids, absorbances of the supernatant at 560 nm were measured [20–23]. Standard curves of hydrolyzed *Sepia* melanin were constructed using 0, 0.1, 0.2, 0.5 and 1 mg ml^{-1} acid-hydrolyzed melanin.

2.4. Wide-angle X-ray diffraction

X-ray powder diffraction studies were carried out on powdered hydroid polyp and the alkaline peroxide cocktail-treated hydroid polyp using a wide-angle X-ray scattering spectrometer equipped with a Cu rotating anode X-ray generator (Rigaku, UltraX18), a double-focusing graded multilayer monochromator and a Mar345 image plate area detector. The beam size at the sample position is 1 mm × 1 mm. Diffraction patterns were corrected for background by acquiring a blank pattern under otherwise identical operating conditions.

2.5. Microscopy and element analysis with secondary ion mass spectroscopy (SIMS) and fluorescence microscope

For scanning electron microscopy (SEM), hydroid perisarc was mounted on conductive carbon tabs on SEM posts (Ted Pella, Redding, CA), sputter-coated using a Desk-II coater equipped with a gold/palladium target (Moorestown, NJ) and imaged in a scanning electron microscope (Vega Ts 5130 mm, Tescan, Czech Republic). Perisarc of *A. latirostris* was embedded in Epofix (Electron Microscopy Sciences, Hatfield, PA) and longitudinally microtomed using a diamond knife. The elemental analysis in the longitudinal sections on a Physical Electronics 6650 Dynamic secondary ion mass spectroscope (Physical Electronics, Chanhassen, MN) was done using a 8 kV oxygen (O^{2+}) beam when collecting depth profiles and a 25 kV gallium (Ga^{+}) beam with a spot size of about 0.5 μm when mapping elemental distribution. The same section was also viewed under 340–400 nm UV light using fluorescence microscopy with a blue filter to see the blue autofluorescence from DOPA and melanin [25]. To evaluate the metal content of the perisarc, the perisarcs were submitted to inductively coupled plasma (ICP) spectroscopy. The ICP used for this study was an IRIS advantage (Thermo Elemental, Franklin, MA). The perisarc was directly preserved under a vacuum after freeze-dried and before analysis to minimize contact with air.

2.6. Raman spectroscopic studies

Perisarc of *A. latirostris* was embedded in PEG-2000 (Carl Roth Gmbh), and 20 μm thick longitudinal sections were microtomed. The perisarc sections were washed thoroughly with several changes in distilled water to remove any remaining PEG, positioned on a quartz slide in distilled water and fixed under a quartz cover slip. For Raman microspectroscopy, a continuous laser beam was focused on the sample through a confocal Raman microscope (model CRM200, WITec, Ulm, Germany) equipped with a piezoelectric scanner (model P-500, PhysikInstrumente, Karlsruhe, Germany). Diode-pumped 785 nm near-infrared laser excitation (Toptica Photonics AG, Graefelfing, Germany) was used in combination with a 100 μm oil-immersed (Nikon, NA = 1.25) microscope objective. Laser power ranging between 15 and 30 mW was used for all measurements. The spectra were acquired with a thermoelectrically CCD (DU401ABV, Andor, Belfast, North Ireland) behind a grating (300 g mm^{-1}) spectrograph (Acton, Princeton Instruments Inc., Trenton, NJ, USA) with a 6 cm^{-1} spectral resolution. Software Scan Ctrl Spectroscopy Plus (version 1.38, Witec) was used for measurement setup. Raman spectra were processed and analyzed with Witec Project Plus software (Version 2.02).

3. Results

3.1. General characterization

Freshly harvested *A. latirostris* hydroids exhibit a brown color (Fig. 1A). The feather-like sprigs with hydroid egg capsules arising from a rachis are colonies of polyps. The proximal of a rachis are typically anchored to marine substrata by a specialized underwater adhesive. Whole polyps are ensheathed by a stiff perisarc. Previously studied chemical composition analysis of *Obelia longissima* hydroid polyp indicated that the *Obelia* perisarc was composed of chitin (~45%), proteins (~40%) and minerals (~10%), by dry weight [26]. Here, the chemical composition of the *Aglaophenia* perisarc was determined (Table 1). The organic and inorganic contents of the initial dry mass of the *Aglaophenia* perisarc were ~98 and ~2 wt.%, respectively. The carbohydrate, protein and lipid contents of the initial dry mass of the sample were ~11, 17 and ~2 wt.%,

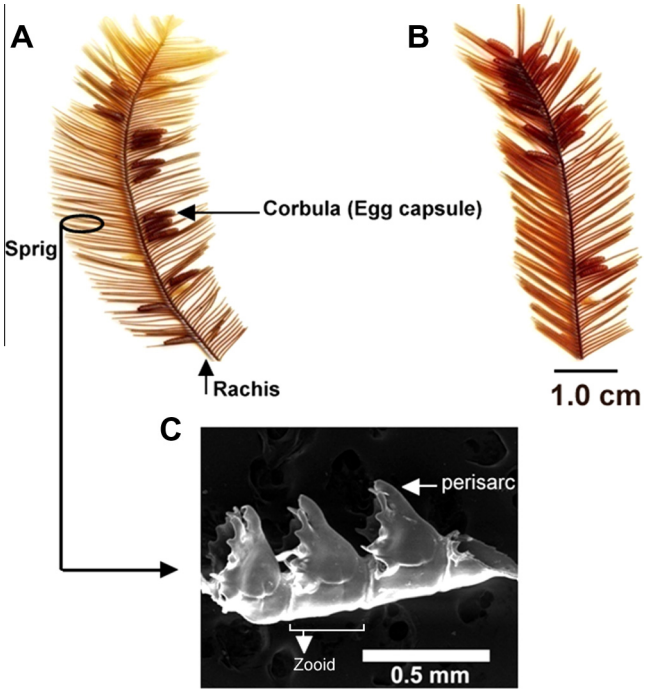

Fig. 1. (A) Marine hydroid *A. latirostris*; (B) hydroid stained for DOPA (Arnow stain); (C) SEM image of sprig showing three zooids.

Table 1
Biochemical composition (in wt.%) in the *Aglaophenia* perisarc.

Organic				Inorganic	Total
Protein	Carbohydrate	Lipid	Melanin		
18.0 ± 2.1 (16.8 ± 8.7)	11.2 ± 1.0 (11.1 ± 1.0)	1.9 ± 2.5	60 ± 6.0	1.5 ± 1.7	~100

The protein content is based on the Lowry method. The values in parentheses are attributed to chitin. Each value represents the mean of three analyses and its standard deviation.

respectively, which significantly do not add up to 98% (Table 1). The protein content analyses in the perisarc studied independently by AA analysis and the Lowry method agree at ~17 wt.%. The chitin content of the sample dry mass measured by the AA analysis was ~11 wt.%, implying most of the carbohydrate in the perisarc is chitin. However, ~70 wt.% of the starting mass of the perisarc remained to be accounted for by further analysis.

3.2. Non-hydrolyzable part characterization

Because 70 wt.% of the *Aglaophenia* perisarc was non-hydrolyzable by acid hydrolysis and only 25 wt.% of the initial mass remained after treatment with alkaline peroxide cocktails [9], we speculated that some portion of the unknown mass might be related to melanin-like pigment because melanin is stable to acid hydrolysis but is degraded by H_2O_2 treatment at alkaline pH and elevated temperatures. The alkaline H_2O_2 treatment with melanin produces pyrrolecarboxylic acids, which absorb at 560 nm [21,22,24]. The fraction of melanin-like pigment in *Aglaophenia* perisarc was estimated to be 60 wt.% based on a *Sepia* melanin standard made by alkaline peroxide cocktails. To confirm the presence of melanin, the non-hydrolyzed sample was collected and quantified after alkaline peroxidation. Interestingly, melanin content based on the detection method was ~87.5 wt.% of the

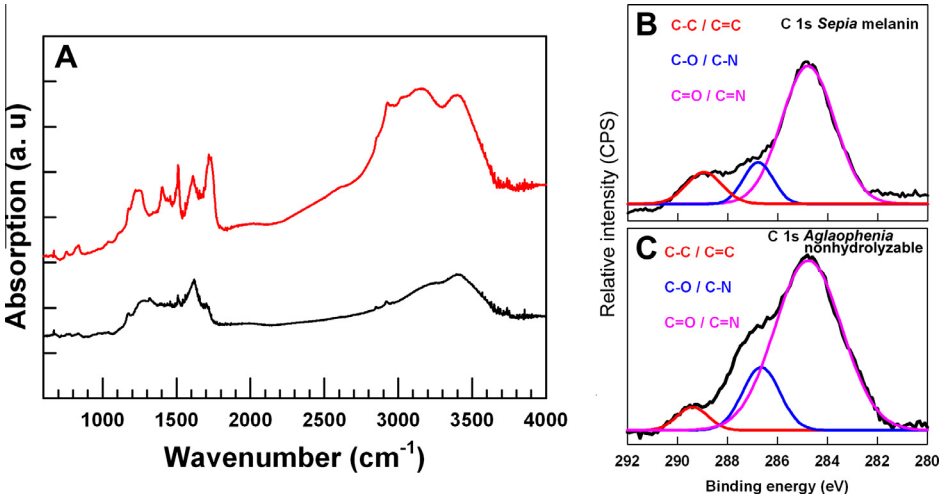

Fig. 2. (A) FTIR adsorption of hydrolyzed *Aglaophenia* perisarc (top) and hydrolyzed *Sepia* melanin (bottom). Band assignments are: peak (3400 cm^{-1}), phenolic-OH stretches; peak (2950 cm^{-1}) aliphatic stretches, CH3 and CH2; peak (1600–1650 cm^{-1}), aromatic C=C stretches, COO stretches; peak (1380–1400 cm^{-1}), phenolic COH bends, indolic and phenolic NH stretches; peak (1260 cm^{-1}), phenolic COH stretches. XPS spectra of (B) *Sepia* melanin and (C) *Aglaophenia* non-hydrolyzable pellet.

non-hydrolyzed sample. As different melanin standards vary in their chemical degradation during alkaline peroxidation, *Sepia* melanin may not be the ideal standard for quantifying perisarc melanin-like pigment. However, this result suggests that the non-hydrolyzed component of the perisarc is mainly composed of melanin-like pigment.

To confirm that the non-hydrolyzable part is mainly composed of melanin-like pigment, FTIR spectroscopy and XPS were performed on the perisarc (Fig. 2). The results showed that the FTIR spectrum for hydrolyzed *Aglaophenia* perisarc resembles that of the control hydrolyzed *Sepia* melanin. A broad band corresponding to phenolic OH stretches was seen at 3400 cm^{-1}; aromatic C=C stretches and COO stretches were identified at 1600–1650 cm^{-1} and phenolic COH stretches were visible at 1260 cm^{-1}, which fit well with the vibrations established in previous studies [20]. The XPS of hydrolyzed *Aglaophenia* perisarc (XPS, Fig. 2B) corroborates the existence of the melanin revealed by FTIR and alkaline peroxide treatment. The XPS spectra of the hydrolyzed *Sepia* melanin and the hydrolyzed *Aglaophenia* perisarc are almost identical in peak type.

Table 2
Amino acid composition of hydroid corbula, sprig and rachis after 1 h hydrolysis.

	Corbula	Sprig	Rachis
Asx	11.1	9.4	10.5
Thr	5.4	4.7	4.1
Ser	7.9	10.2	6.2
Glx	10.0	10.0	7.3
Pro	6.1	6.7	4.5
Gly	18.7	19.3	26.4
Ala	6.8	5.7	5.7
Cys	1.7	0.9	1.4
Val	3.8	3.9	4.6
Met	1.0	1.8	0.6
Ile	1.9	1.5	1.8
Leu	1.9	2.0	2.1
DOPA			
Tyr	2.0	2.5	3.7
Phe	2.3	1.9	1.7
His	5.4	2.1	1.5
Lys	7.9	6.1	7.6
Arg	10.0	5.8	6.0
Total	94.7	94.5	95.7

Each value represents the mean of three analyses.

3.3. AA analysis and wide-angle X-ray diffraction of Aglaophenia perisarc

Glycine is the dominant AA in the proteins of hydroid perisarc (~20 mol.%) based on the AA composition analysis (Table 2, Fig. 3). Histidine, present at >10 mol.% levels in both squid beak and polychaete jaws, was less than 2 mol.% in the perisarc [1,4,7,8]. Another intriguing compound detected by the AA composition analysis was a broad peak at 40 min corresponding to glucosamine (Fig. 3). Because glucosamine is a product formed during the acid hydrolysis of chitin, it was expected that chitin content in the perisarc would be relatively high. Indeed, total chitin content in perisarc was deduced from AA composition analysis to be about 11 wt.% of the perisarc. The X-ray diffraction (XRD) spectrum of the perisarc powder also supported the existence of chitin fiber crystalline phase in the perisarc due to a similarity with a spectrum of α-chitin from crab shell (Fig. 4) [11,27]. However, it is unclear whether the crystalline phase is α-chitin or β-chitin [28] because XRD obtained from the perisarc powder contains other organic and inorganic materials and the chitin content is less than 11 wt.%.

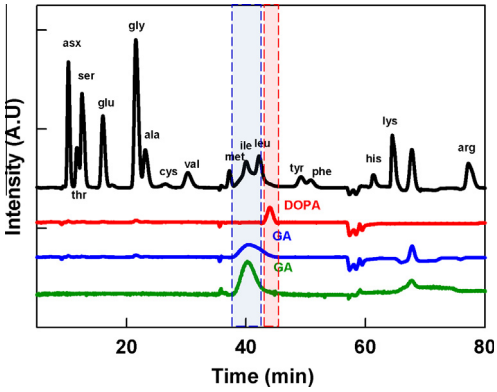

Fig. 3. Amino acid analysis profiles of hydroid perisarc-derived DOPA and glucosamine. Acid-hydrolyzed mature dry hydroid perisarc is shown in black, DOPA purified by affinity chromatography from hydrolyzed perisarc is shown in red, a glucosamine purified from hydrolyzed perisarc following alkaline peroxidation is shown in blue and a glucosamine standard is shown in green.

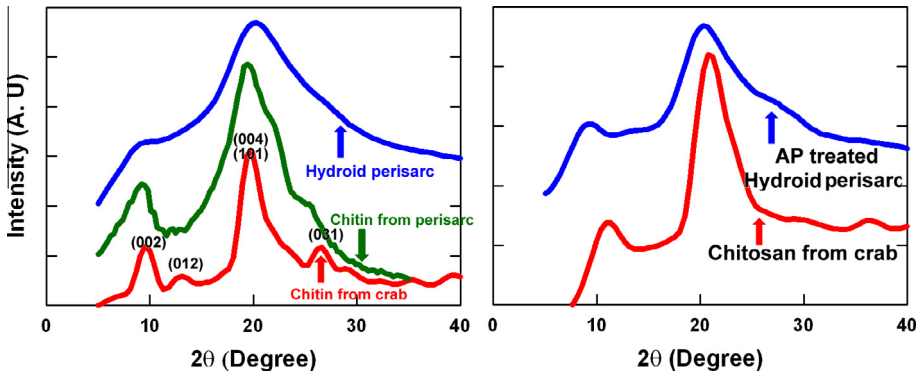

Fig. 4. Wide-angle X-ray diffraction spectra for pooled homogenized hydroid perisarc (left, blue curve), chitin purified from hydroid perisarc (left, green curve) and alkaline peroxidation cocktail treated hydroid perisarc (right, blue curve). Chitin and chitosan from crab were used as controls.

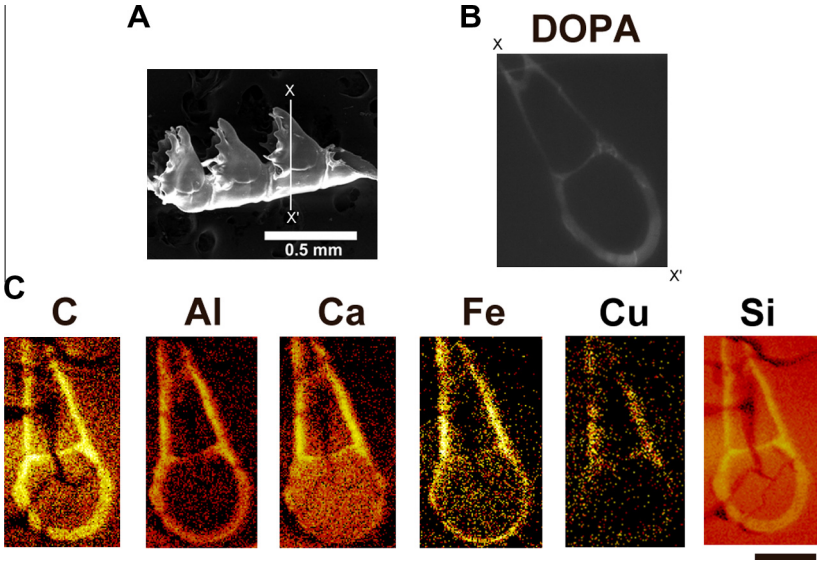

Fig. 5. Chemical analysis of a hydroid zooid. (A) SEM (orientation of X-section as indicated); (B) intrinsic fluorescence of thin section (λ of excitation = 340–400 nm and detected by blue filter); (C) SIMS of the thin section shown in B (scale bar = 100 μm).

3.4. Catechol identification in Aglaophenia perisarc

A catechol, dopamine, was reported in previous analyses of *Laomedea* and *Obelia longissima* hydroid polyps [14,15]. To explore the catechol (*o*-diphenol) presence in *Aglaophenia* perisarc, the Arnow assay was performed. *Aglaophenia* perisarc, like previously studied *Laomedea* perisarc, stained red when treated with Arnow reagent (positive for catechols, Fig. 1B), confirming the presence of catechol derivatives. However, the intensity of the red color developed by the Arnow reagent was weaker than mussel byssus (personal observation), suggesting that the concentration of catechol derivatives in hydroids is lower than in mussel byssus. To identify catecholic compounds, the perisarc was hydrolyzed and the derived catecholic compounds were separated and purified by phenyl-borate affinity chromatography. The fraction purified by the phenyl-borate column was analyzed by ESI-MS and AA analysis. Interestingly, the only catecholic compound detected, based on AA analysis and ESI-MS, was DOPA, not dopamine as previously reported in other hydroid species (Fig. S1) [13,14]. The DOPA content of whole perisarc obtained by AA analysis following acid hydrolysis is likely obscured by a large, broad glucosamine peak, the end-product of chitin hydrolysis in the perisarc (Fig. 3). The proximal end of a rachis, where the hydroid polyp holdfast is tethered to the substratum, was also stained red with Arnow, implying that the hydroid may utilize DOPA in underwater adhesive proteins, as mussels and sandcastle worms do. Whole hydroids were homogenized in 8 M urea/5% acetic acids, then the supernatant was separated in acid–urea polyacrylamide gel electrophoresis gel and stained with Coomassie blue R and nitroblue tetrazolium (NBT) to detect DOPA-containing protein (Fig. S2) [29]. A cluster of NBT-positive bands are detected and provide evidence for the existence of DOPA-containing protein in the hydroids. DOPA can affect the biological materials by many different pathways, such as melanization, cross-link formation and metal ion binding [30,31].

3.5. Element analysis in Aglaophenia perisarc

A transverse cross-section of hydroid zooid (X–X′) was viewed under 340–400 nm UV light by fluorescence microscopy and element image mode by SIMS (Fig. 5). As shown in Fig. 5A, the cross-sectioned perisarc exhibited a blue-green fluorescence. Because melanin and DOPA from the identified perisarc components have blue-green fluorescence (λ_{em} 400–500 nm), DOPA and/or melanin may be distributed in the perisarc. Elemental maps of the sections generated by SIMS revealed that iron, calcium, silicon, aluminum

Table 3
Total concentrations of aluminum, calcium, iron and silicon from the *Aglaophenia* perisarc.

Element	Al	Ca	Fe	Si
Concentration (mg)/ perisarc (g)	0.49 ± 0.01	2.17 ± 0.64	0.49 ± 0.01	0.89 ± 0.01

Each value represents the mean of three analyses and its standard deviation.

and a trace of copper are localized in the perisarc. To determine the amount of metal detected by SIMS, whole perisarcs were measured in ICP. As shown in Table 3, the metals quantified in the perisarc were Si (0.089 wt.%), Al (0.049 wt.%), Ca (0.23 wt.%) and Fe (0.049 wt.%) (Table 3). Compared with standard seawater, hydroid perisarcs have six times as much Ca and 10^4 times as much Fe [32]. Cu was not detected at all and the Zn content was 0.02 wt.%.

3.6. Confocal resonance Raman microscopy of Aglaophenia perisarc cross-section

The catechol moiety of DOPA exhibits a high affinity for metal ions and metal oxides, e.g. Fe^{3+} with cumulative log stabilities (i.e. log K_s) of 37–40 [33,34]. The colocalization and complexation of Fe and DOPA in the mussel byssal coating are responsible for its extraordinary combination of high hardness and high extensibility [35–37]. Therefore, we speculated that DOPA residues in the *Aglaophenia* perisarc may form some coordination complexes with the iron in the perisarc. Spectroscopic research to find the evidence for metal complexation with DOPA was thus performed.

Confocal resonance Raman microscopy is a powerful tool to map the distribution of DOPA–Fe coordination complexes in tissues. The reason for resonance lies in the characteristic charge transfer absorption associated with transfer of nonbonding π DOPA electrons to Fe^{3+} in DOPA–Fe complexes in the near-infrared region of the electromagnetic spectrum. By applying near-infrared laser line, only protein–metal coordination sites will be enhanced and visible in the Raman spectrum. This method was successfully utilized to localize DOPA–Fe complexation in the protective cuticles of mussel byssal threads [35] and plaques [37]. Fig. 6 shows the results of Raman spectroscopic imaging on a thin (20 μm) section of the hydroid perisarc. An optical micrograph of the analyzed region is shown in Fig. 6A, whereas Fig. 6B shows two representative resonance Raman spectra of hydroid perisarc (blue and red line). Both spectra are dominated by specific Fe^{3+}–DOPA complexation bands (500–650 cm^{-1}) and the DOPA ring vibrations (1380–1520 cm^{-1}). The two spectra differ mainly in the intensity ratios of the peaks, which could be due to the variety of coordination sites in the cuticle. The spectral features observed resemble those observed in mussel byssus coating (black line). Fig. 6C–E shows the results of Raman spectroscopic imaging of the same section integrated for different regions of the spectra: namely, overall fluorescence, Fe^{3+}–DOPA complexation and CH stretching. Notably, DOPA–Fe coordination is present throughout the whole perisarc, suggesting DOPA and its complex with iron(III) as a possible contributor to the as yet untested mechanical properties of perisarc.

4. Discussion

Squid beaks and polychaete jaws, which consist primarily of nonmineralized macromolecules, have attracted attention in part because their remarkable hardness and stiffness are more

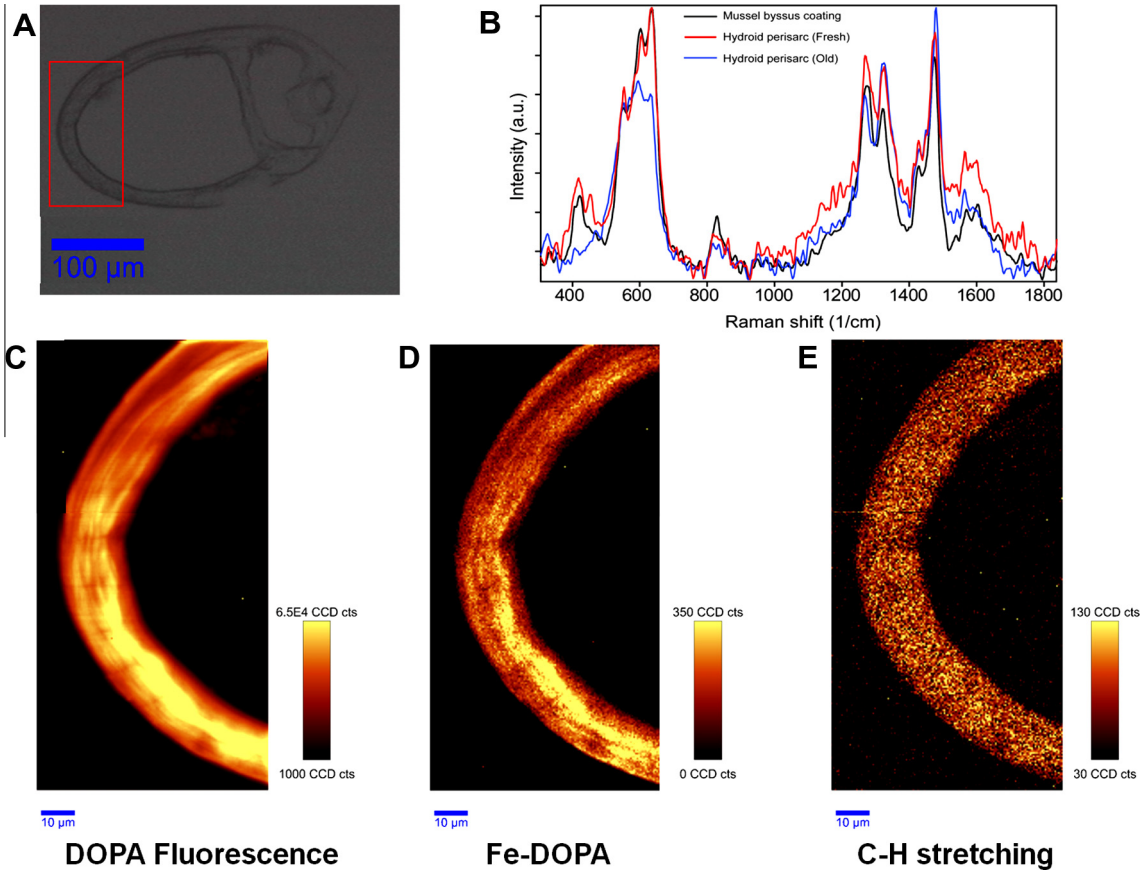

Fig. 6. Confocal resonance Raman microscopy of perisarc. (A) Optical image of a section of hydroid with perisarc indicated by a box; (B) Raman spectra of fresh (red) and old (blue) perisarc sections using a laser excitation of 785 nm;(C-E) Raman imaging of the same perisarc section indicated in A integrated over three different wavenumber ranges: (C) overall fluorescence (50-3400cm^{-1}), (D) Fe–DOPA complexation (490-696 cm^{-1}) and (E) C-H stretching (2850-3010cm^{-1}).

comparable with ceramics than with known organic polymers [5]. Chitin [3,11], melanin [2,9] and Fe^{3+}–DOPA coordination complexes [30,34,36] are proposed to be combined in some way, to endow the perisarc of the hydroid *Aglaophenia* with the toughness needed for survival in the very exposed intertidal zone.

Chitin (N-acetyl-D-glucosamine connected by β linkages), found in the *Aglaophenia* perisarc, is a structural polysaccharide found in the hard tissues of many other marine invertebrates (e.g. squids, crabs, shrimps and sea spiders). The reported stiffness of chitin nanofibers is at least 150 GPa [13,38], and is much greater than the stiffness of wet regenerated chitin films prepared in ionic liquids (<0.5 GPa; unpublished data). Indeed, in *Dosidicus* squid beak, which has a chitin-based supporting frame [3], the stiffness of 5 GPa at the distal tip with less than ~20 wt.% water decreases significantly to 30 MPa at the proximal wing with more than 70 wt.% water content [3,12]. Therefore, control of hydration around the chitin composite is one of the key challenges to tuning the stiffness of the composite under wet conditions.

Condensation of oxidized catechols with histidine-rich proteins was identified as a key mechanism for controlled water content in the squid beak [3,12]. Similarly, catechols (DOPA), pigment and a chitinous supporting frame were identified in the *Aglaophenia* perisarc. However, the most dominant difference was low histidine content (<2%) in the perisarc, in contrast with the jumbo squid beak histidine content (~10 wt.%) [11], suggesting that DOPA–His cross-links are unlikely to be a coupling pathway in perisarc. Rather, the high fraction of melanin-like pigment (~60%) in the perisarc was suggested by XPS, IR and alkaline peroxide treatment. Most biological integuments generally have less than 5% dry weight of melanin, which functions primarily as a colorant and sunscreen. In contrast, the melanin of polychaete *Glycera* jaw (~37% dry weight) has a distinct load-bearing function, and contributes to about half of the observed hardness and stiffness of this structure [2,9,39]. The chemical identification of melanin is never a trivial task, hence caution is called for in interpreting the present results. On the one hand, analysis of the reaction of perisarc with alkaline peroxidation and acid hydrolysis suggests a eumelanin-like composition for *Aglaophenia* pigments; on the other hand, in situ Raman microscopy of perisarc failed to detect melanin resonances consistent with the *Sepia* melanin standard. In the case of squid beak, significant melanin was actually an artifact formed post-hydrolytically by the oxidation and polymerization of catechol adducts freed from the cross-linked structure [12]. A similar artifact is probable from a DOPA- and Fe^{3+}-rich material, as we suppose perisarc to be. Indeed, Mentasti and Pelizzetti [40] have shown that catechols are highly prone to pigment formation in the presence of Fe^{3+} at acidic pH.

Based on the experimental results and discussion above, we propose the pigment in *Aglaophenia* perisarc to have two functions: (i) to enhance the cohesiveness of the perisarc; and (ii) to help control hydration by acting as a hydrophobic coating around the perisarc. Indeed, the formation of pigment around a chitosan (the deacetylated form of chitin) film not only increases the hydrophobicity of the film but also enhances the film's tensile properties under wet conditions to a level comparable to that of the chitosan film in dry conditions by reducing the hydration and swelling of chitosan due to water adsorption [41]. Melanins are also known to bind metal ions via their hydroxyl and carboxyl functionalities [42–44]. Copper has the highest binding affinity to eumelanin. Indeed, copper ion is also bound to the melanin of the *Glycera* jaw and has a significant influence on the mechanical performance of the jaw. Even though copper was not detected in ICP analysis of the *Aglaophenia* perisarc, melanins can form coordination complexes with other metal ions [42–44]. From the ICP analysis result, Fe, Ca, Si and Al were also present in the perisarc, suggesting that chelates or salt bridges are probably formed between the macromolecules and those ions.

Biological materials can use covalent and non-covalent cross-linking between their building blocks to enhance cohesion. As the biological material becomes more cross-linked, it is less susceptible to swelling, and is denser and stiffer. Extensive covalent cross-links in keratin, mediated by its cysteine residues, and in collagen, mediated by lysine and hydroxylysine, are well known factors affecting cohesion [45,46]. Recently, noncovalent cross-links mediated by metal coordination have attracted attention as alternative sclerotizing strategies. Owing to the presence of zinc and manganese, the hardness of spider fangs and teeth was enhanced twofold compared to bulk mandible [47]. Zinc–histidine coordination in polychaete *Nereis* jaw and iron–DOPA complex in mussel *Mytilus* byssal cuticles also contribute to their extraordinary mechanical properties [8,35].

Similar to mussel adhesive plaque, we observed the *Aglaophenia* perisarc to possess 10^4 times more iron than ambient standard seawater, as well as a DOPA-containing protein and Fe^{3+}–DOPA complexes with nearly identical resonance Raman spectral shifts and intensities. The catechol functionality of DOPA exhibits a strong binding affinity for Fe^{3+} with cumulative log stabilities (i.e. log K_s) of 37–40 [33]. The mechanochemistry of Fe^{3+}–DOPA mediated cross-links is reversible yet robust, roughly comparable to the binding of well-oriented biotin–avidin interactions [31]. Fe^{3+}–DOPA complexes in the mussel thread cuticle are correlated with an epoxy-like stiffness and a rubbery extensibility [35]. Therefore, correlating the mechanical properties of *Aglaophenia* perisarc with the distribution of Fe^{3+}–DOPA complexes is of considerable interest for future research. Similarly, the range of achievable properties in materials made by combining chitin, DOPA, Fe^{3+} and other metal ions needs to be explored systematically.

DOPA is also a covalent cross-linker. For example, after oxidation to DOPA quinone, reverse dismutation of DOPA with quinone forms di-DOPA cross-links [48]. The reaction intermediates from the oxidation of DOPA (e.g. DOPA quinone and dopachrome) can be covalently coupled to the amine group of D-glucosamine in chitin fibers and can mediate cross-linking between chitin fibers. DOPA–thiol covalent crosslinks [19] are also likely to form because energy-dispersive X-ray analysis on the perisarc showed the high intensity of characteristic sulfur X-rays (Fig. S3).

The presence of chitin, DOPA, Fe^{3+} and a high molecular weight pigment in *Aglaophenia* perisarc is intriguing because no marine biomaterials are known to combine all four components in the same tissue. *Dosidicus* squid beak has only chitin and DOPA [11], *Mytilius* (mussel) byssus has only DOPA and Fe^{3+} [25] and *Glycera* jaw has only melanin [2,9]. The role of DOPA and DOPA-mediated cross-linking in *Dosidicus* squid beak was linked with the dehydration of chitin, thereby maintaining strong mechanical properties of chitin in water. On the other hand, catecholate–Fe^{3+} complexes in the byssal thread cuticle are correlated with its peculiar rigid yet extensible tensile properties. The existence of a DOPA-containing protein and Fe^{3+}–DOPA chelate complex in the perisarc suggests the possibility of chemical and mechanical parallels to both the mussel byssal cuticle and the squid beak, and need to be explored further.

5. Conclusions

We investigated the perisarc of the marine hydroid *A. latirostris* to understand how nature designs a stiff, tough and lightweight sheathing structure. Chitin and a melanin-like pigment constitute 10 and 60 wt.% of the perisarc, respectively, but less than 2 wt.% can be attributed to inorganic elements. Interestingly, a DOPA-containing protein and iron were identified in the perisarc, which

suggests a similarity to the adhesive and coating of mussel byssal threads. A resonance Raman spectrum due to DOPA–iron(III) complex formation was also detected in the perisarc, implying the existence of DOPA–iron(III) interaction associated with chitin and melanin-like structures. Analysis of the surfaces of perisarc sections, perisarc architecture and the ultrastructural arrangement of the components remain to be done. In addition, the chemical interactions between various components of the perisarc should be studied.

Acknowledgements

This work was supported by Marine Biomaterials Research Center under Marine Biotechnology Program, Ministry of Oceans and Fisheries Affairs, Korea. We thank Ms. Son Min-Hui for ESI-MS analysis.

Appendix A. Supplementary data

Supplementary data associated with this article can be found, in the online version, at http://dx.doi.org/10.1016/j.actbio.2013.06.015.

Appendix B. Figures with essential color discrimination

Certain figures in this article, particularly Figs. 1–7, are difficult to interpret in black and white. The full color images can be found in the on-line version, at http://dx.doi.org/10.1016/j.actbio.2013.06.015.

References

[1] Lichtenegger HC, Schoberl T, Bartl MH, Waite H, Stucky GD. High abrasion resistance with sparse mineralization: copper biomineral in worm jaws. Science 2002;298:389–92.
[2] Moses DN, Mattoni MA, Slack NL, Waite JH, Zok FW. Role of melanin in mechanical properties of *Glycera* jaws. Acta Biomater 2006;2:521–30.
[3] Miserez A, Schneberk T, Sun C, Zok FW, Waite JH. The transition from stiff to compliant materials in squid beaks. Science 2008;319:1816–9.
[4] Lichtenegger HC, Schoberl T, Ruokolainen JT, Cross JO, Heald SM, Birkedal H, et al. Zinc and mechanical prowess in the jaws of Nereis, a marine worm. Proc Natl Acad Sci U S A 2003;100:9144–9.
[5] Broomell CC, Khan RK, Moses DN, Miserez A, Pontin MG, Stucky GD, et al. Mineral minimization in nature's alternative teeth. J R Soc Interface 2007;4:19–31.
[6] Broomell CC, Zok FW, Waite JH. Role of transition metals in sclerotization of biological tissue. Acta Biomater 2008;4:2045–51.
[7] Broomell CC, Chase SF, Laue T, Waite JH. Cutting edge structural protein from the jaws of Nereis virens. Biomacromolecules 2008;9:1669–77.
[8] Broomell CC, Mattoni MA, Zok FW, Waite JH. Critical role of zinc in hardening of Nereis jaws. J Exp Bio 2006;209:3219–25.
[9] Moses DN, Harreld JH, Stucky GD, Waite JH. Melanin and Glycera jaws: emerging dark side of a robust biocomposite structure. J Biol Chem 2006;281:34826–32.
[10] Khan RK, Stoimenov PK, Mates TE, Waite JH, Stucky GD. Exploring gradients of halogens and zinc in the surface and subsurface of Nereis jaws. Langmuir 2006;22:8465–71.
[11] Miserez A, Li Y, Waite JH, Zok F. Jumbo squid beaks: inspiration for design of robust organic composites. Acta Biomater 2007;3:139–49.
[12] Miserez A, Rubin DJ, Waite JH. Cross-linking chemistry of squid beak. J Biol Chem 2010;285:38115–24.
[13] Nishino T, Matsui R, Nakamae K. Elastic modulus of the crystalline regions of chitin and chitosan. J Polym Sci B 1999;37:1191–6.
[14] Knight DP. Sclerotization of the perisarc of the calyptoblastic hydroid, Laomedea flexuosa. 1. The identification and localization of dopamine in the hydroid. Tissue & Cell 1970;2:467–77.
[15] Knight DP. Sclerotization of the perisarc of the calyptoblastic hydroid, Laomedea flexuosa. 2. Histochemical demonstration of phenol oxidase and attempted demonstration of peroxidase. Tissue & Cell 1971;3:57–64.
[16] Knight DP. Cellular basis for quinone tanning of the perisarc in the thecate hydroid Campanularia (=Obelia) flexuosa Hinks. Nature 1968;218:584–6.
[17] Marsh JB, Weinstein DB. Simple charring method for determination of lipids. J Lipid Res 1966;7:574–6.
[18] Arnow L. Colorimetric determination of the components of 3,4-dihydroxyphenylalanine–tyrosine mixtures. J Biol Chem 1937;118:531–7.
[19] Zhao H, Sun C, Stewart RJ, Waite JH. Cement proteins of the tube-building polychaete Phragmatopoma californica. J Biol Chem 2005;280:42938–44.
[20] Glass K, Ito S, Wilby PR, Sota T, Nakamura A, Bowers CR, et al. Direct chemical evidence for eumelanin pigment from the Jurassic period. Proc Natl Acad Sci U S A 2012;109:10218–23.
[21] Ito S, Wakamatsu K, Ozeki H. Spectrophotometric assay of eumelanin in tissue samples. Anal Biochem 1993;215:273–7.
[22] Ozeki H, Ito S, Wakamatsu K, Thody AJ. Spectrophotometric characterization of eumelanin and pheomelanin in hair. Pigment Cell Res 1996;9:265–70.
[23] Wakamatsu K, Nakanishi Y, Miyazaki N, Kolbe L, Ito S. UVA-induced oxidative degradation of melanins: fission of indole moiety in eumelanin and conversion to benzothiazole moiety in pheomelanin. Pigm Cell & Melanoma Res 2012;25:434–45.
[24] Napolitano A, Pezzella A, Vincensi MR, Prota G. Oxidative-degradation of melanins to pyrrole acids – a model study. Tetrahedron 1995;51:5913–20.
[25] Holten-Andersen N, Mates TE, Toprak MS, Stucky GD, Zok FW, Waite JH. Metals and the integrity of a biological coating: the cuticle of mussel byssus. Langmuir 2009;25:3323–6.
[26] Tretenichenko EM, Datsun VM, Ignatyuk LN, Nud'ga LA. Preparation and properties of chitin and chitosan from a hydroid polyp. Russ J Appl Chem 2006;79:1341–6.
[27] Carlstrom D. The crystal structure of alpha-chitin (poly-N-acetyl-D-glucosamine). J Biophys Biochem Cytol 1957;3:669–83.
[28] Blackwell J. Structure of beta-chitin or parallel chain systems of poly-beta-(1–4)-N-acetyl-D-glucosamine. Biopolymers 1969;7:281–98.
[29] Waite JH. Precursors of quinone tanning. Methods Enzymol 1995;258:1–20.
[30] Rubin DJ, Miserez A, Waite H. Diverse of protein sclerotization in marine invertebrates: structure–property relationship in natural biomaterials. Adv Insect Physiol 2010;3:139–49.
[31] Zeng H, Hwang DS, Israelachvili JN, Waite JH. Strong reversible Fe^{3+}-mediated bridging between dopa-containing protein films in water. Proc Natl Acad Sci U S A 2010;107:12850–3.
[32] Sun C, Waite JH. Mapping chemical gradients within and along a fibrous structural tissue, mussel byssal threads. J Biol Chem 2005;280:39332–6.
[33] Taylor SW, Chase DB, Emptage MH, Nelson MJ, Waite JH. Ferric ion complexes of a DOPA-containing adhesive protein from Mytilus edulis. Inorg Chem 1996;35:7572–7.
[34] Lee H, Scherer NF, Messersmith PB. Single-molecule mechanics of mussel adhesion. Proc Natl Acad Sci U S A 2006;103:12999–3003.
[35] Harrington MJ, Masic A, Holten-Andersen N, Waite JH, Fratzl P. Iron-clad fibers: a metal-based biological strategy for hard flexible coatings. Science 2010;328:216–20.
[36] Holten-Andersen N, Fantner GE, Hohlbauch S, Waite JH, Zok FW. Protective coatings on extensible biofibres. Nat Mater 2007;6:669–72.
[37] Hwang DS, Zeng H, Masic A, Harrington MJ, Israelachvili JN, Waite JH. Protein- and metal-dependent interactions of a prominent protein in mussel adhesive plaques. J Biol Chem 2010;285:25850–8.
[38] Vincent JGV, Wegst GK. Design and mechanical properties of insect cuticle. Arthropod Struct Dev 2004;33:187–99.
[39] Moses DN, Pontin MG, Waite JH, Zok FW. Effects of hydration on mechanical properties of a highly sclerotized tissue. Biophys J 2008;94:3266–72.
[40] Mentasti E, Pelizzetti E. Reaction between iron (III) and catechol (o-dihydroxybenzene). Part I. Equilbria and kinetics of complex formation in aqueous acid solution. J Chem Soc Dalton Trans 1973:2605–8.
[41] Oh DX, Hwang DS. A biomimetic chitosan composite with improved mechanical properties in wet conditions. Biotechnol Prog, **29**, 2013, 505-512.
[42] Froncisz W, Sarna T, Hyde JS. Cu2+ probe of metal-ion binding sites in melanin using electron paramagnetic resonance spectroscopy. I. Synthetic melanins. Arch Biochem Biophys 1980:202.
[43] Sarna T, Froncisz W, Hyde JS. Cu2+ probe of metal-ion binding sites in melanin using electron paramagnetic resonance spectroscopy. II. Natural melanins. Arc Biochem Biophys 1980;22:202.
[44] Zucca FA, Giaveri G, Gallorini M, Albertini A, Toscani M, Pezzoli G, et al. The neuromelanin of human substantia nigra: physiological and pathogenic aspects. Pigm Cell Res 2004;17:610–7.
[45] Kagan HM. Characterization and regulation of LO. Orlando, FL: Academic Press; 1986.
[46] Menefee E. Physical and chemical consequences of keratin crosslinking, with application to the determination of crosslink density. Adv Exp Med Biol 1977;86A:307–27.
[47] Schofield R, Lefevre H. High-concentrations of zinc in the fangs and manganese in the teeth of spiders. J Exp Bio 1989;144:577–81.
[48] Burzio LA, Waite JH. The other Topa: formation of 3,4,5-trihydroxyphenylalanine in peptides. Anal Biochem 2002;306:108–14.